

## Electronic Supplementary Information

### **Honeycomb-like Fe/Fe<sub>3</sub>C-doped porous carbon with more Fe-N<sub>x</sub> active sites for promoting the electrocatalytic activity of oxygen reduction**

Guiming Wu,<sup>a</sup> Chunfeng Shao,<sup>b</sup> Boyang Cui,<sup>a</sup> Hailiang Chu,<sup>\*a</sup> Shujun Qiu,<sup>\*a</sup> Yongjin Zou,<sup>a</sup> Fen Xu<sup>a</sup> and Lixian Sun<sup>\*a</sup>

<sup>a</sup> *Guangxi Key Laboratory of Information Materials, Engineering Research Center of Ministry of Education for Electronic Information Materials and Devices, and School of Materials Science and Engineering, Guilin University of Electronic Technology, Guilin, 541004, People's Republic of China*

<sup>b</sup> *Key Laboratory of Fuel Cell Technology of Guangdong Province, School of Chemistry and Chemical Engineering, South China University of Technology, Guangzhou 510640, People's Republic of China*

*\* Authors for correspondence*

*Email: chuhailiang@guet.edu.cn (H. Chu)*

*qiushujun@guet.edu.cn (S. Qiu)*

*sunlx@guet.edu.cn (L. Sun)*

*Tel.: +86-773-2216607*

*Fax: +86-773-2290129*

## Materials

$\text{Zn}(\text{C}_2\text{H}_3\text{OO})_2 \cdot 2\text{H}_2\text{O}$  and  $\text{Fe}(\text{NO}_3)_3 \cdot 9\text{H}_2\text{O}$  were purchased from Xilong Chemical Co., Ltd. 2-methylimidazole and methanol were obtained from Macklin. 2, 6-diaminopyridine(DAP) was purchased from Aladdin. Commercial 40 wt% Pt/C catalyst was purchased from Johnson Matthey Corporation. All chemicals used in this work are analytically pure without further purification.

## Preparation of ZIF-8

ZIF-8 was synthesized by following a reported route with some minor modifications.<sup>S1</sup> In a typical procedure, 16.42 g of 2-methylimidazole and 4.39 g of  $\text{Zn}(\text{C}_2\text{H}_3\text{OO})_2 \cdot 2\text{H}_2\text{O}$  were respectively dissolved in 300 mL methanol and stirred for 1 h. The above two solutions were quickly mixed and the mixed solution was continuously stirred for 12 h at room temperature. Subsequently, the resulting white solid was centrifuged and washed three times with methanol. Finally, the sample was dried under vacuum at 60 °C overnight to obtain ZIF-8 powder.

## Preparation of Catalysts

In a typical synthesis procedure of nFe-DPC (n represents the percentage of iron content), 0.6 g of ZIF-8 was dispersed into 10 mL ethanol and the mixture was sonicated for 30 minutes to obtain homogeneous mixture. Then 2.8 mL of 0.05 M  $\text{Fe}(\text{NO}_3)_3 \cdot 9\text{H}_2\text{O}$  (m = 56.5 mg) was introduced dropwise. After stirring for ten minutes, 0.5 g of DAP was added and the resulting mixture was continuously stirred and evaporated for 12 h at room temperature. Subsequently, the resultant dark green slurry was further subjected to vacuum drying at 50 °C for 8 h. Finally, the finely grounding powder was placed in a tube furnace, which was carbonized at 950 °C at a heating rate of 5 °C/min and kept for 3 h under a flowing nitrogen gas. The resulting sample of 5Fe-DPC was obtained. Other samples of nFe-DPC with different iron contents (n = 0, 0.5, 2.5 and 10) were prepared under the same procedures except for the different Fe contents.

For comparison, some control samples of 5Fe-ADPC and 5Fe-PC were prepared. For 5Fe-ADPC, 5Fe-DPC was acidized in 0.5 M  $\text{H}_2\text{SO}_4$  for 8-10 h, then washed with ultrapure water and ethanol. After vacuum drying at 60 °C, 5Fe-ADPC was obtained

after calcination at 950 °C for 1 h. For 5Fe-PC, the preparation process was basically the same as that of 5Fe-DPC. After adding 1.5 mL of 0.05 M  $\text{Fe}(\text{NO}_3)_3 \cdot 9\text{H}_2\text{O}$  dropwise into 0.6 g of ZIF-8 ethanol dispersion solution, rotary evaporation at room temperature for 12 h was followed by vacuum drying at 50 °C for 8 h. Finally, the sample was subjected to the same heating treatment process as 5Fe-DPC to obtain 5Fe-PC.

## Characterizations

Scanning electron microscopy (SEM, Quanta 450 FEG) and transmission electron microscopy (TEM, Talos F200X and Tecnai G2 F30 S-TWIN) are used to observe the morphology and microstructure of the catalysts. The crystal structure of the catalysts was analyzed by using Bruker D8 Advance X-Ray Diffractometer with Cu K $\alpha$  radiation ( $\lambda = 1.5418 \text{ \AA}$ , 40 kV, 40mA). The graphitization degree of the catalysts was characterized by the Renishaw Invia Raman Microscope System with a 532 nm laser beam (Labram HR Evolution, Horiba JY, France). After the catalysts were degassed in vacuum at 90 °C for 1 h and 250 °C for 8 h, nitrogen sorption isotherms were obtained by Nitrogen adsorption by Surface Area and Porosity Analyzer at 77 K. The specific surface area (SSA) and pore size distribution (PSD) curves were calculated by Brunauer-Emmett-Teller (BET) formula and Barrett-Joyner-Halenda (BJH) desorption model, respectively. X-ray photoelectron spectroscopy (XPS, Thermo Scientific Escalab 250Xi) was used to study the valence states of the elements on the surface of catalysts. Inductively coupled plasma optical emission spectroscopy (ICP-OES, America Agilent ICPOES730) was used to determine the content of Fe.

## Electrochemical measurements

All the electrochemical tests of the catalysts were carried out by using a multi-channel electrochemical workstation (Ivium, Netherlands). At room temperature of 25( $\pm$ 1) °C, a three-electrode electrochemical system was used for testing, which is consisted of a rotating ring-disk glass carbon electrode (RDE, 5 mm in diameter) as the working electrode substrate, Hg/HgO (1 M KOH) electrode as the reference electrode and platinum wire as counter electrode. Before using the Hg/HgO reference electrode, it was calibrated according to the reversible hydrogen electrode (RHE). Using platinum wire as the working electrode, the cyclic voltammograms test was carried out in a 0.1 M KOH solution saturated with ultrapure hydrogen at a scan rate of 1 mV s<sup>-1</sup>. The average values of the two electrode potentials when the current crossed zero were obtained as the calibration potential according to Figure S1:  $E_{\text{RHE}} = E_{\text{Hg/HgO}} + 0.898 \text{ V}$ .

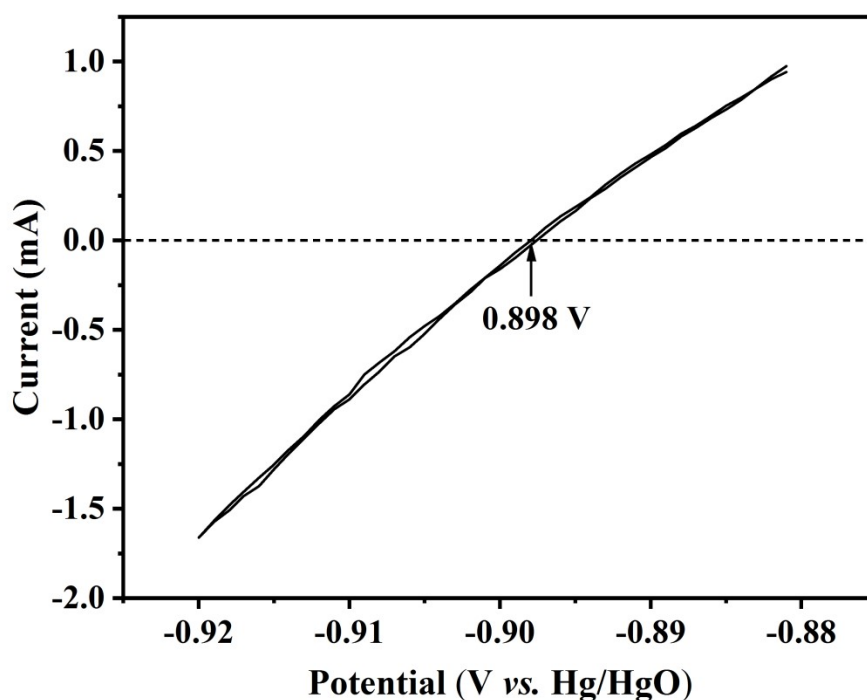


Figure S1. CV curve of the Hg/HgO reference electrode at a scan rate of  $1 \text{ mV s}^{-1}$  in  $\text{H}_2$ -saturated  $0.1 \text{ M KOH}$ .

To prepare the working electrode, 4 mg of the as-prepared catalyst was ultrasonically dispersed in 1 mL of Nafion/ethanol solution (0.25 wt% Nafion). Then, after about 40 min of ultrasonic treatment, 20  $\mu\text{L}$  of catalyst ink was dropped on the glassy carbon electrode and dried naturally at room temperature. The catalyst loading was determined to be  $0.4 \text{ mg cm}^{-2}$ . For comparison, commercial 40 wt% Pt/C catalyst was prepared in the same way, with a catalyst loading of  $50 \text{ ug Pt cm}^{-2}$ . Linear Sweep Voltammogram (LSV) and Cyclic Voltammogram (CV) tests of all the catalysts were carried out at a sweep rate of  $10 \text{ mV/s}$  in nitrogen or oxygen-saturated  $0.1 \text{ M KOH}$  electrolyte. The long-term stability of catalysts was determined by current-time (i-t) chronoamperometric responses at  $0.60 \text{ V vs. RHE}$  with a stirring speed of 1600 rpm. The ORR transfer electron number (n) is calculated by the Koutecky-Levich formula:

$$\frac{1}{J} = \frac{1}{B\omega^{1/2}} + \frac{1}{J_K} \quad (1)$$

$$B = 0.62nF(D_0)^{2/3}\nu^{-1/6}C_0 \quad (2)$$

where  $J$  and  $J_K$  are the measured and kinetic current densities, respectively,  $\omega$  is the angular velocity of the electrode,  $n$  is the number of electron transfers at the working electrode, and  $F$  represents the Faraday constant ( $96,485 \text{ C mol}^{-1}$ ).  $D_0$  is the diffusion coefficient of oxygen-saturated in the electrolyte,  $C_0$  is the concentration of oxygen-saturated in the electrolyte,  $\nu$  is the viscosity of the electrolyte (when  $0.1 \text{ M KOH}$  electrolyte is used,  $D_0 = 1.9 \times 10^{-5} \text{ cm}^2 \text{ s}^{-1}$ ,  $C_0 = 1.2 \times 10^{-5} \text{ cm}^2 \text{ s}^{-1}$ ,  $\nu = 1.0 \times 10^{-2} \text{ cm}^2 \text{ s}^{-1}$ ).

### **Zn-air Battery assembly and measurement**

Typically, 5Fe-DPC, zinc powder (0.27 g), glass fiber and 6 M KOH containing 0.2 M zinc acetate are used as cathode catalyst, anode, separator and electrolyte, respectively. For comparison, the commercial 40 wt% Pt/C catalyst is also tested in Zn-air battery. Dispersing 5 mg of catalyst and 40  $\mu\text{L}$  of Nafion (5%) in a mixed solution of 1 mL of ethanol and water (1:1, V/V) to obtain a uniform ink by ultrasonication for 30 min. The resulting ink is then uniformly loaded on Ni foam and carbon paper with gas diffusion layer. After natural drying, the air cathode is obtained with loading 5Fe-DPC catalyst of  $\sim 4 \text{ mg cm}^{-2}$  or 40 wt% Pt/C of  $\sim 0.75 \text{ mg cm}^{-2}$ . Zn-air batteries are tested using a two-electrode system (CR2025 coin cell). The polarization curves are performed on a CHI660E electrochemical working station. The galvanostatic discharge is conducted by Neware battery testing system (CT-4008).

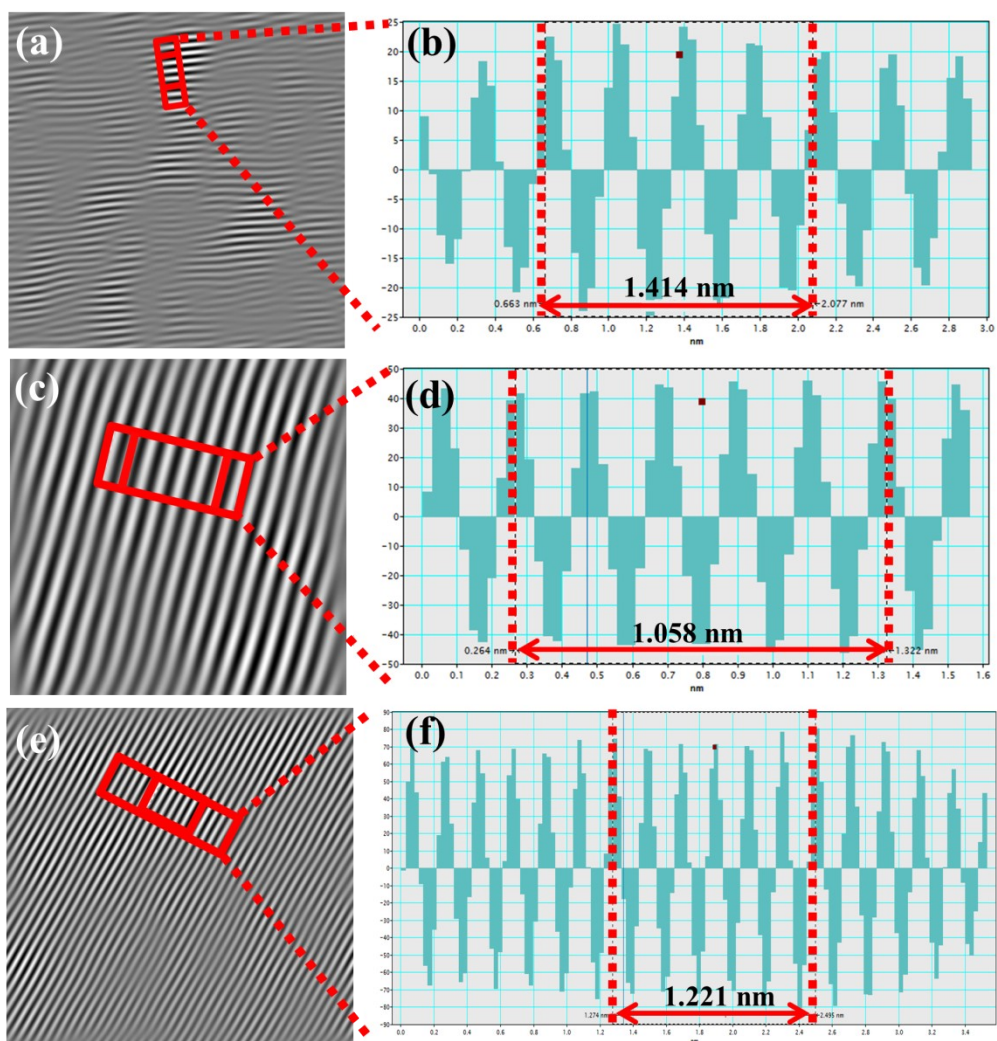


Figure S2. Determination of the spacing of crystalline lattices from HRTEM images in 5Fe-DPC for (a and b) carbon layer, (c and d) Fe<sub>3</sub>C and (e and f) Fe nanoparticles.

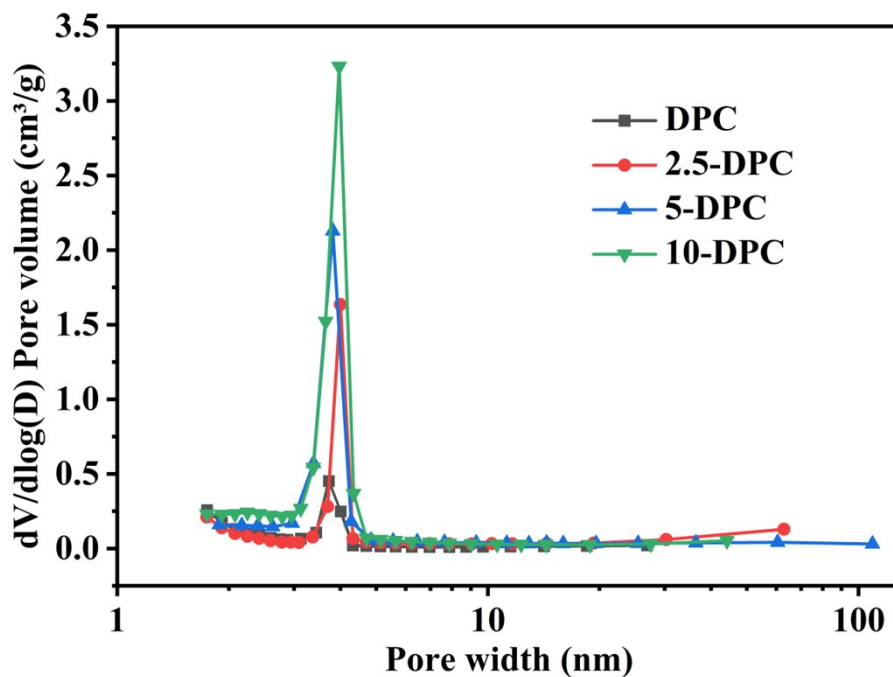


Figure S3. Pore size distributions of DPC and nFe-DPC (n=2.5, 5 and 10).

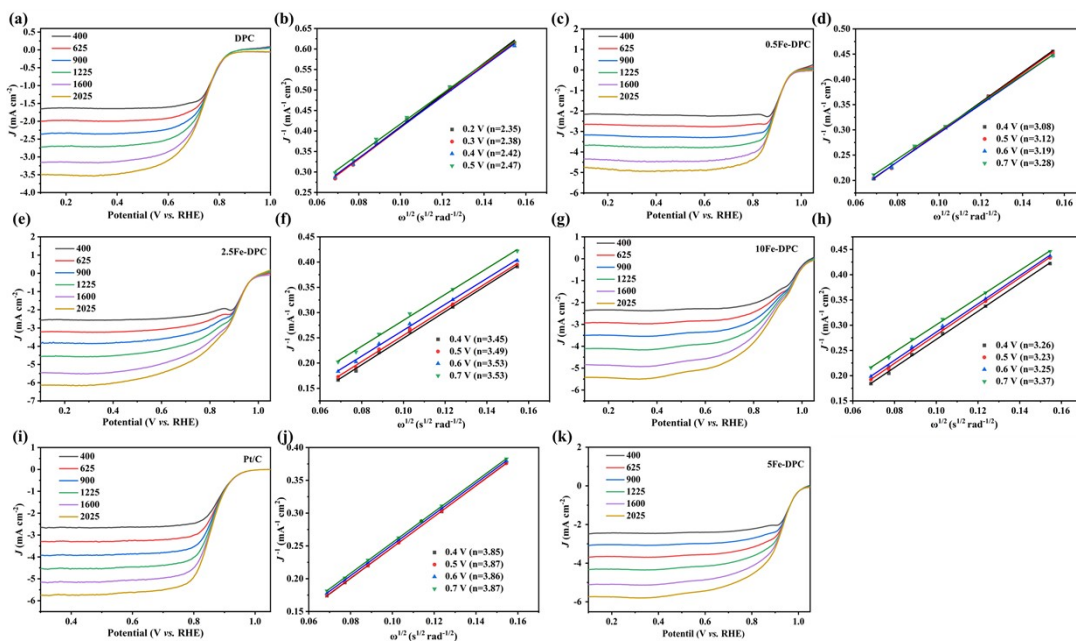


Figure S4. (a, c, e, g, I and k) LSV curves of DPC, nFe-DPC (n=0.5, 2.5, 5 and 10) and 40 wt% Pt/C in O<sub>2</sub>-saturated 0.1 M KOH solution with different stirring speeds; (b, d, f, h and j) K-L plots of DPC, nFe-DPC (n=0.5, 2.5, and 10) and 40 wt% Pt/C.



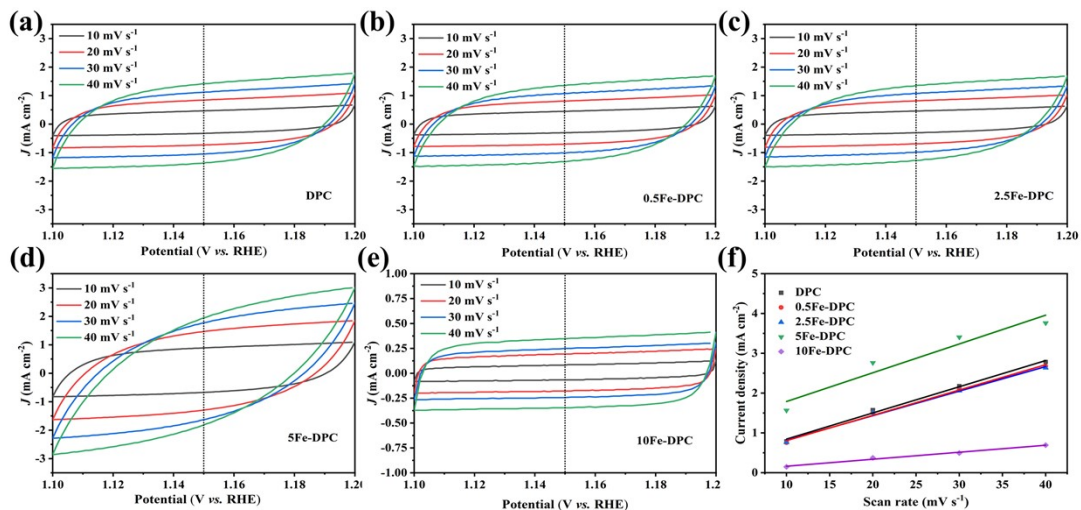


Figure S5. (a-e) Cyclic voltammetry of catalysts in  $N_2$ -saturated in 0.1 M KOH; (f) Relationship between scan rate and current density at 1.15 V vs. RHE of catalysts.

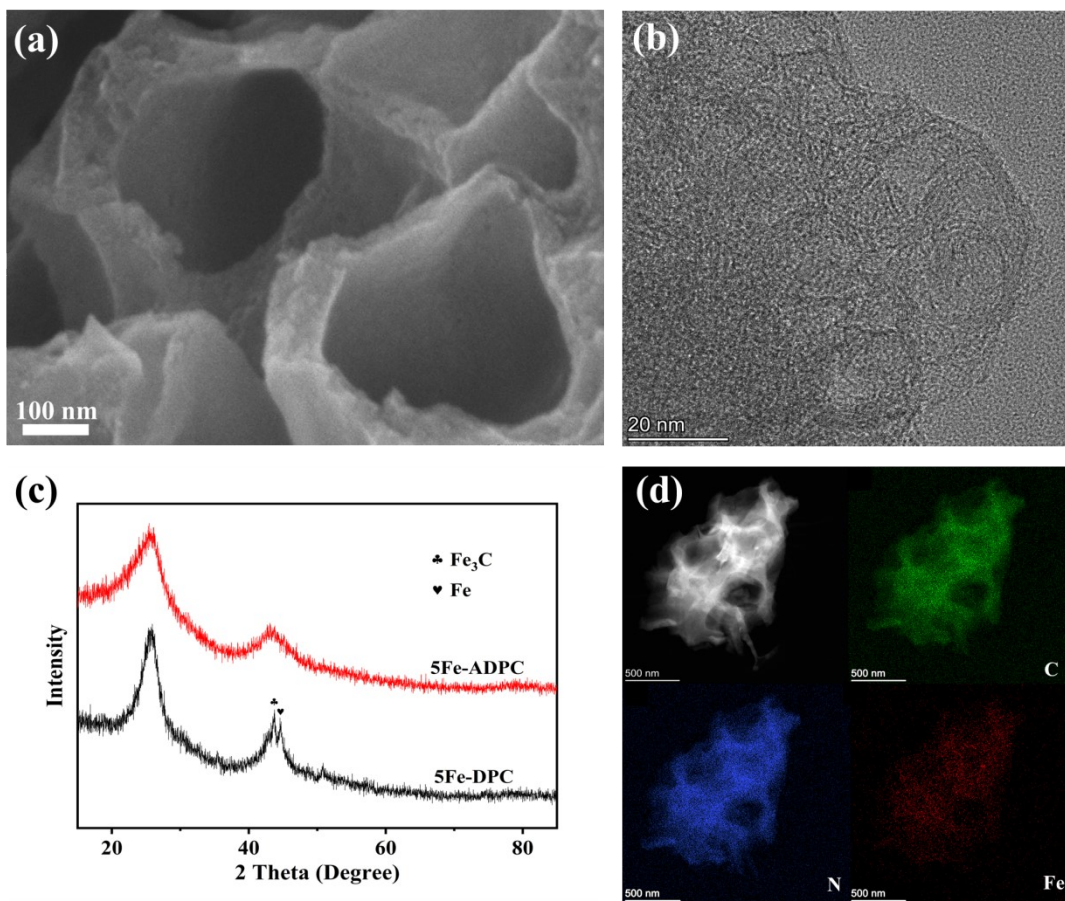


Figure S6. (a-b) SEM and HRTEM image of 5Fe-ADPC; (c) XRD patterns of 5Fe-ADPC and 5Fe-DPC; (d) HADDF-STEM image and elemental mapping of 5Fe-ADPC.

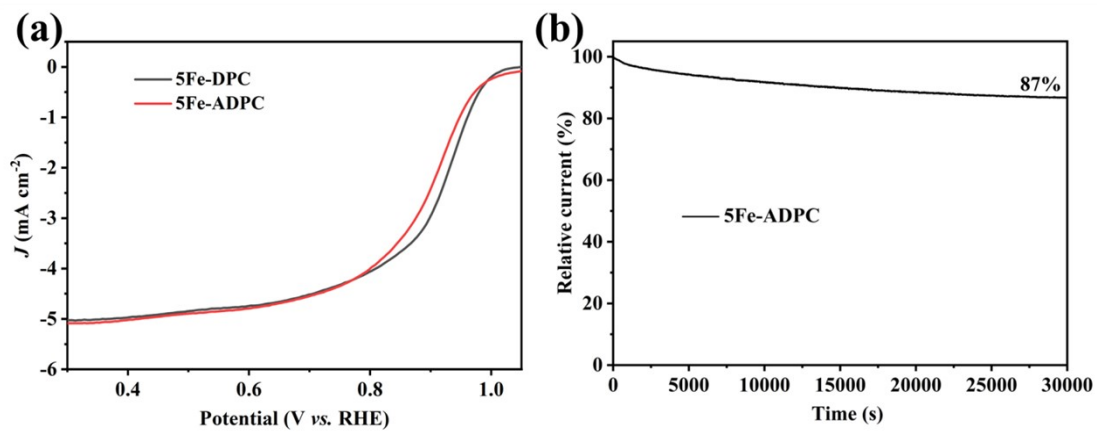


Figure S7. (a) LSV curves of 5Fe-ADPC and 5Fe-DPC catalysts in O<sub>2</sub>-saturated 0.1 M KOH solution with a sweep rate of 10 mV/s; (b) chronoamperometric response for the 5Fe-ADPC at 0.6 V in O<sub>2</sub>-saturated 0.1 M KOH (1600 rpm).

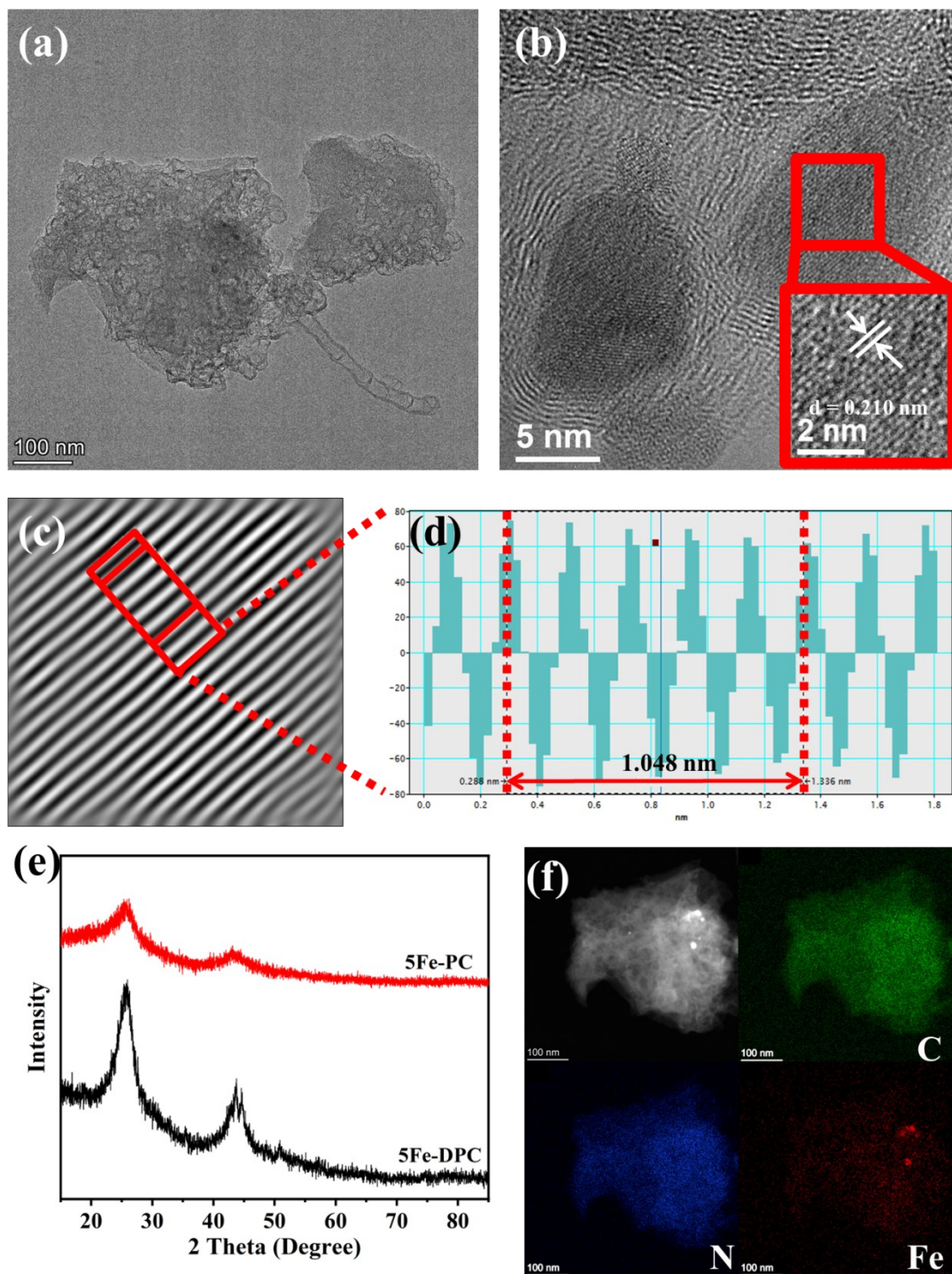


Figure S8. (a and b) TEM and HRTEM images of 5Fe-PC; (c and d) Determination of the spacing of crystalline lattices from HRTEM images in 5Fe-PC; (e) XRD patterns of 5Fe-PC and 5Fe-DPC; (f) HADDF-STEM image and elemental mapping of 5Fe-PC.

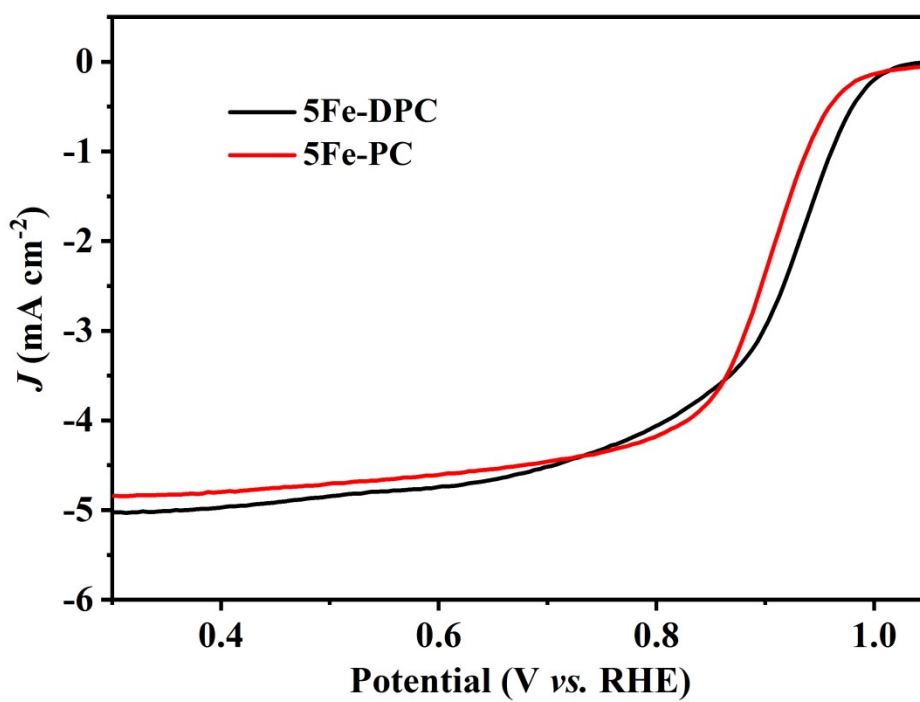


Figure S9. LSV curves of 5Fe-PC and 5Fe-DPC catalysts in  $\text{O}_2$ -saturated 0.1 M KOH solution with a sweep rate of 10 mV/s.

**Table S1** Textural properties of the DPC and nFe-DPC electrocatalysts.

Samples	Specific surface area [m <sup>2</sup> g <sup>-1</sup> ]				V <sub>Adsorption</sub> [cm <sup>3</sup> g <sup>-1</sup> ]	APD <sup>e</sup> [nm]
	S <sub>total</sub> <sup>a</sup>	S <sub>micro</sub> <sup>b</sup>	S <sub>ext</sub> <sup>c</sup>	ratio <sup>d</sup>		
DPC	559.71	464.51	95.20	83.0%	0.33	2.3
2.5Fe-DPC	615.09	499.65	115.44	81.2%	0.43	2.8
5Fe-DPC	508.96	305.49	203.47	60.0%	0.39	3.0
10Fe-DPC	450.79	170.59	280.20	37.8%	0.40	3.5

<sup>a</sup> The total specific surface area (SSA).

<sup>b</sup> The micropore area.

<sup>c</sup> The external surface area.

<sup>d</sup> The proportion of micropore surface area in total SSA.

<sup>e</sup> The average pore diameter.

**Table S2** Elemental composition attained from XPS and Fe contents were measured by ICP-OES.

Samples	XPS (at%)			Fe content (wt%)
	Fe	N	C	
2.5Fe-DPC	0.95	8.20	90.86	2.49
5Fe-DPC	0.85	5.65	93.5	4.66
10Fe-DPC	0.80	4.53	94.67	6.39
5Fe-ADPC	-	-	-	2.69

**Table S3** The relative ratio and atomic content of the deconvoluted N group were analyzed based on XPS.

Samples	Pyridinic N		Fe-N		Pyrrolic N		Graphitic N		Oxide N	
	[%]	[at%]	[%]	[at%]	[%]	[at%]	[%]	[at%]	[%]	[at%]
2.5Fe-DPC	39.98	3.28	5.07	0.42	8.98	0.74	23.66	1.94	22.31	1.83
5Fe-DPC	32.29	1.82	5.73	0.32	13.57	0.77	26.37	1.49	22.04	1.24
10Fe-DPC	22.27	1.01	3.96	0.18	6.01	0.27	36.05	1.63	31.7	1.44

**Table S4** Comparison of the ORR activities for 5Fe-DPC with recently reported Fe-N-C catalysts in 0.1 M KOH aqueous solution.

Catalysts	$E_{\text{onset}}$	$E_{1/2}$	$E_{1/2}(\text{Pt/C})$	References
<b>5Fe-DPC</b>	1.01	0.92	0.86	<b>This work</b>
<b>Fe-AC-2</b>	1.0	0.87	0.85	J. Mater. Chem. A, 2021, 9, 7137-7142.
<b>Fe-NHC</b>	0.94	0.89	0.83	Appl Catal B-Environ, 2021, 285, 119780.
<b>Fe<sub>3</sub>C-FeN/NC</b>	0.95	0.80	---	J. Mater. Chem. A, 2021, 9, 6831-6840.
<b>FC-900</b>	0.973	0.847	0.845	Appl Catal B-Environ, 2021, 284, 119721.
<b>Fe-N-HMCTs</b>	0.992	0.872	0.858	Adv Funt Mater, 2021, 31, 2009197.
<b>Fe-N-C</b>	0.99	0.89	0.86	J Power Sources Advances, 8, 2021, 100052.
<b>Fe-N-NDC-1-900</b>	1.06	0.89	0.86	J. Mater. Chem. A, 2021, 9, 5556-5565.
<b>Fe SA-NSC-900</b>	0.94	0.86	0.85	ACS Energy Lett, 2021, 6, 379-386.
<b>SA-Fe-NHPC</b>	1.01	0.93	0.85	Adv Mater, 2020, 32, 1907399.
<b>3DOM Fe-N-C-900</b>	---	0.875	0.845	Nano Energy, 2020, 71, 104547.
<b>Fe-SCNS</b>	---	0.89	0.85	Angew Chem Int Edit, 2020, 44, 19627-19632.
<b>FeNC-950</b>	0.94	0.84	0.83	J Power Sources, 2020, 450, 227659.
<b>Fe<sub>3</sub>O<sub>4</sub>@FeNC</b>	1.007	0.89	0.854	Carbon, 2020, 162, 245-255.
<b>FeAC@FeSA-N-C</b>	---	0.912	0.897	ACS Nano, 2019, 13, 11853-11862.
<b>Fe SAs/NC</b>	---	0.91	0.842	ACS Catal, 2019, 9, 2158-2163.

## References

- S1 L. L. Zou, C. C. Hou, Q. J. Wang, Y. S. Wei, Z. Liu, J. S. Qin, H. Pang and Q. Xu, *Angew. Chem.-Int. Ed.*, 2020, **59**, 19627-19632.